Robotic Joints and Contact Dynamics Experiments: Lessons Learned from ROKVISS

ASTRA 2006

28 – 30 November 2006 at ESTEC, Noordwijk, the Netherlands

B. Rebele [1], B. Schaefer [1], A. Albu-Schaeffer [1], W. Bertleff[1], K. Landzettel[1]

[1] DLR
Institute of Robotics and Mechatronics
Muenchner Strasse 20
82234 Wessling
Germany
bernhard.rebele@dlr.de

ABSTRACT

Precise knowledge of robotic motion dynamics is a pre-requisite for controller design and successful manipulator in-orbit operations. The system dynamics strongly depend on the friction, damping and stiffness parameters. These physical parameters change with outer space conditions like huge temperature variations and material degradation. Since ROKVISS was installed outside at the Russian Service Module of the International Space Station (ISS) in January 2005, ROKVISS operates successfully as an on-orbit experimental platform. The measurements collected during almost 2 years of operation in space allow drawing reliable conclusions on the robotic joints damping and on the contact forces for interacting surfaces in space. The modeling of the joint friction and the tangential contact forces and the identification of the corresponding parameter is addressed in this paper.

EXPERIMENT DESCRIPTION

ROKVISS is the second space robot experiment realized by DLR's Institute of Robotics and Mechatronics (DLR-RM) in cooperation with the German space companies EADS-ST, Kaiser-Threde, and vHS (von Hoerner & Sulger) with close collaboration of the Russian Federal Space Agency ROSKOSMOS and RKK Energia. In January 2005, approximately three years after the project was started, ROKVISS was mounted outside the Russian Service Module of the International Space Station (Fig. 1).
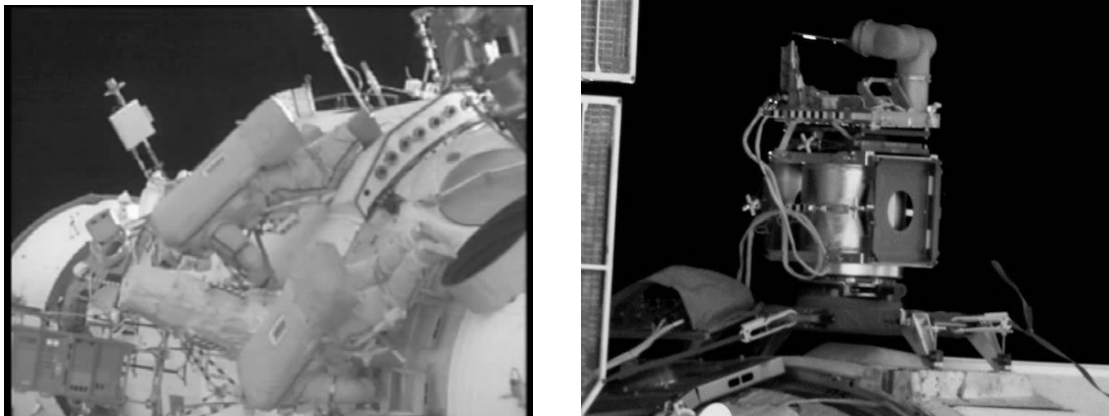

Fig. 1. At the end of a 5 hours space walk the astronauts succeeded in mounting ROKVISS

Since February 2005 ROKVISS is operated by DLR-RM from the German Ground Station in Weilheim, supported by ZUP (ISS ground station in Moscow) and will be continued until February 2007.
ROKVISS consists of a small experimental robot with two joints (Fig. 2) mounted on a Universal Workplate, a controller, a stereo camera, an illumination system, an earth observation camera, a power supply, and a mechanical contour device with two springs. The main goals of ROVVISS [1], [2], [3] are
- The identification of their dynamics, specifically damping and friction behavior over time, in order to update and validate mathematical models and to gain increased confidence in the modelling process, also for more advanced robotized future missions.

- The verification of DLR`s modular light-weight robotic joints in the outer space, under realistic mission conditions.
- The verification of force-reflecting telemanipulation to show the feasibility of telepresence methods [4],[5] for future satellite servicing tasks, as we are convinced that the inclusion of the human ground operator into the control loop is a must in many situations.
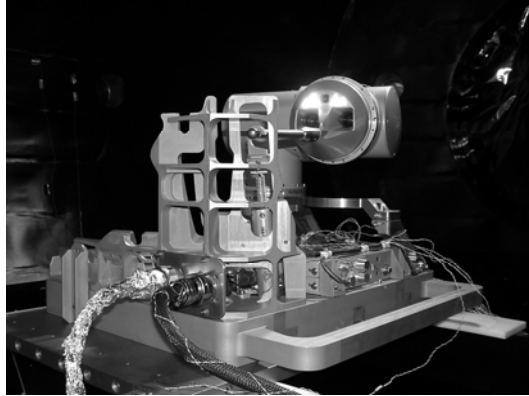

Fig. 2. ROKVISS manipulator with mechanical contour

JOINT PARAMETER IDENTIFICATION

Joint Model

For both joints, the current I, the motor position q and the joint torque τ, measured at the torque sensor, are recorded at a sample rate of 12ms. The joint velocity and acceleration are calculated by differentiation and properly filtering of the measured motor position. Making use of the gear ration, the motor torque τ_m, the motor position q and the motor inertia are transformed to the joints side. The motor torque τ_m is related to I through the motor constant k_m:

$$\tau_m = k_m^{-1} \cdot I \tag{1}$$

Assuming rigid bodies, the dynamic model of the robot joints is given by

$$\tau_m = J \cdot \ddot{q} + \tau + \tau_F \tag{2}$$

where τ_F is the friction torque. The inertia matrix J represents the inertia of the motor, the gear and the link up to the torque sensor. The inertia matrix is obtained by detailed 3D CAD models [6], [7], including motors, gears, electronics and the cabling. For terrestrial applications and lubricants respectively the following friction model, which was initially used, captures the damping behavior of the harmonic drive gear:

$$\tau_F = \left(b_0 + b_{0T} \left|\tau\right|\right) \cdot sign\left(\dot{q}\right) + b_1 \cdot \dot{q} \tag{3}$$

where b_0 and b_{0T} are the parameters of constant and load-dependent Coulomb friction respectively, and b_1 is the viscous damping coefficient.

To excite the friction parameters of (3) properly, the spring of the experimental contour is pulled at constant velocities of 1°/s, 5°/s, 10°/s, 20°/s and 40°/s. The resulting position, velocity and joint torque of this standard identification trajectory, hereafter referred to as 'spring', are shown in Fig. 3.
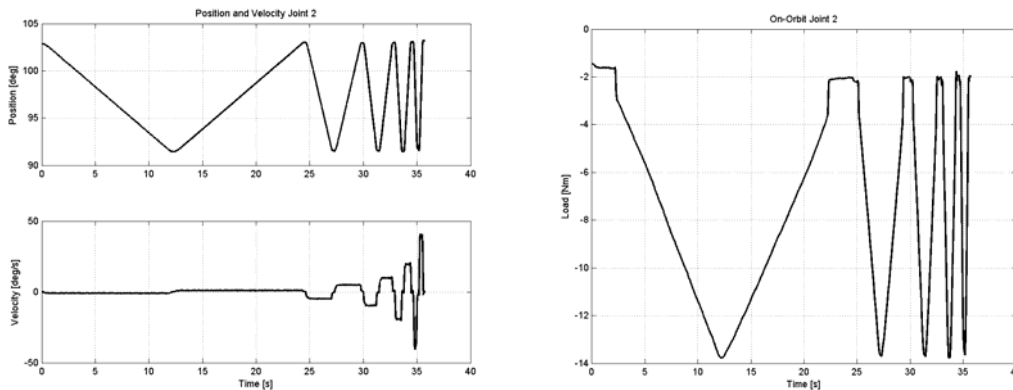

Fig. 3. Typical measurements for standard identification trajectory

Results for Parameter Identification

First measurements on ground showed that the use of the space qualified lubricant changes the friction behavior fundamentally. In Fig. 4 and 5, it can be seen, that a linear viscous damping term does not anymore represent the velocity dependent damping. Introducing a quadratic and cubic friction component with corresponding parameters b_2 and b_3 allows to capture the nonlinear damping behavior much better. The enhanced model, hereafter referred to as cubic model, is given by

$$\tau_F = \left(b_0 + b_{0T}\,|\tau|\right) \cdot sign\left(\dot{q}\right) + b_1 \cdot \dot{q} + b_2 \cdot \dot{q} \cdot |\dot{q}| + b_1 \cdot \dot{q}^3 \tag{4}$$
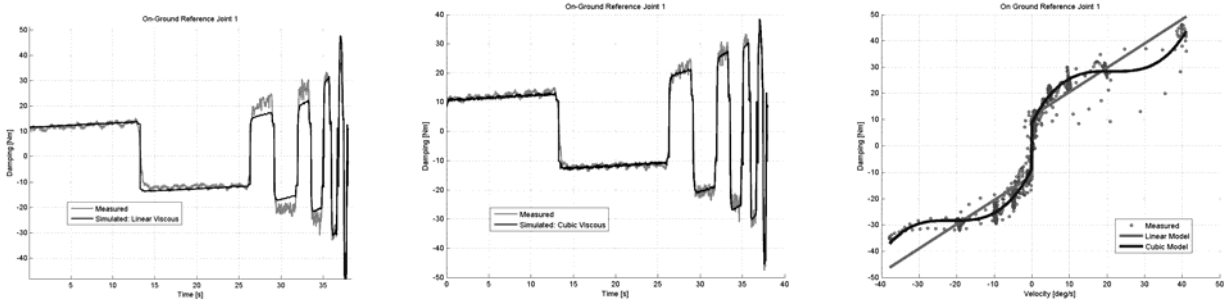

Fig. 4. Joint 1: Measured and simulated damping for the linear (left) and the cubic (middle) model and approximation of nonlinear viscous damping for both models (right)
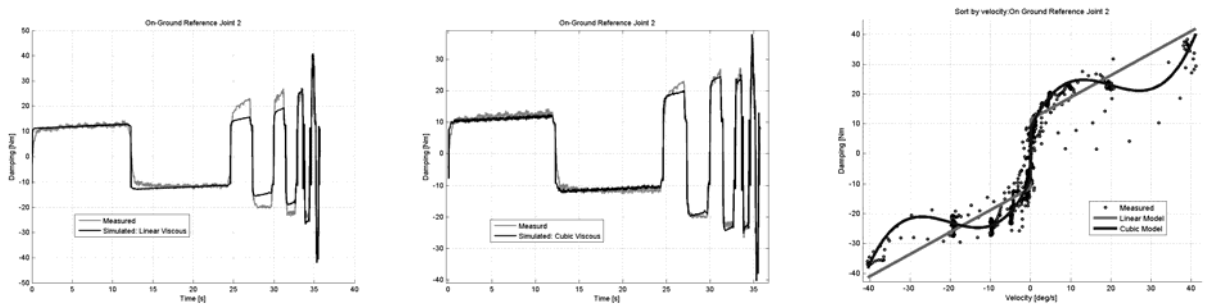

Fig. 5. Joint 2: Measured and simulated damping for the linear (left) and the cubic (middle) model and approximation of nonlinear viscous damping for both models (right)

Exposed to the outer space conditions and compared to the on-ground values, damping increases for both joints from the very beginning. According to Fig. 6, Coulomb friction and damping at low velocity (1°/s) respectively, increases by approximately 100% for joint 1 and 50% for joint 2. Mainly for joint 1, damping continues to increase slowly during the entire mission (see Fig. 7).
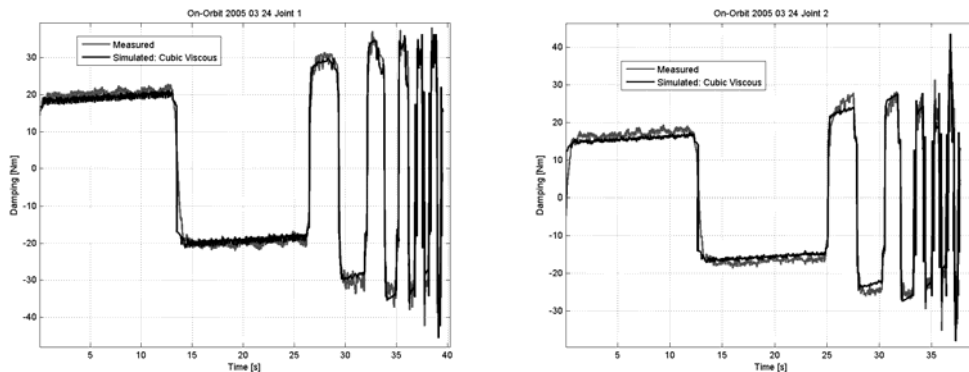

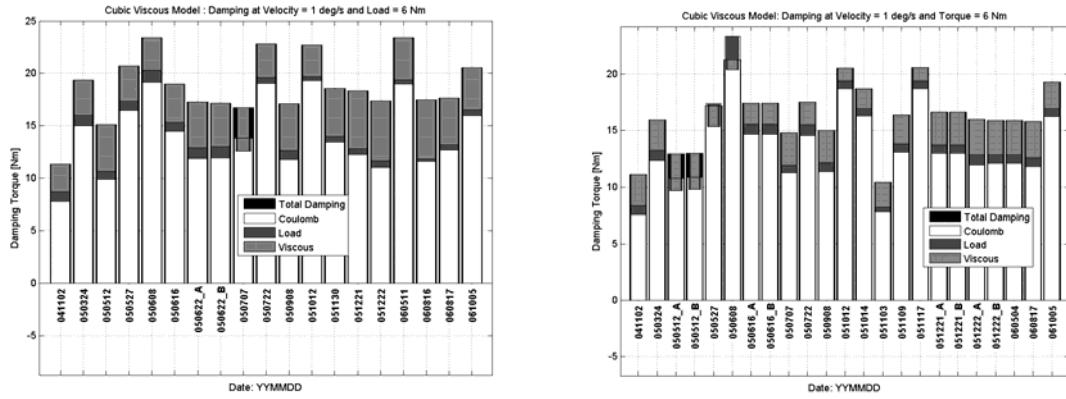Fig. 6. Increased damping in space for joint 1 (left) and joint 2 (right)

Fig. 7. Evaluation of identified damping at low velocity for joint 1 (left) and joint 2 (right)

For all experiments, the two joints showed the nonlinear viscous damping with the characteristic shape depicted in Fig. 8. The parameters identified for a trajectory approximate the damping behavior of a differently shaped trajectory, like the sinusoidal trajectory of Fig. 9 whereas the parameters identified for both trajectories may vary slightly (see Table 1). Depending on the velocity range, different combinations of parameters may be obtained, e.g. the quadratic and cubic damping parameters b_2 and b_3 of the sinusoidal trajectory, without changing the overall damping behavior. In general, due to the higher number of optimization parameters, the variance of complex models over different experiments is higher. It has to be mentioned that the quadratic viscous damping parameter b_2 takes on negative values but does not introduce energy to the system as the three viscous damping terms have to be treated together. For the sinusoidal trajectory, the joint is operated without pulling the spring and the applied joint torque is therefore negligible. The load dependent parameter b_{0T} is not properly excited and therefore not identified, and set to zero respectively.

Table 1. Friction Parameters identified for Joint 2

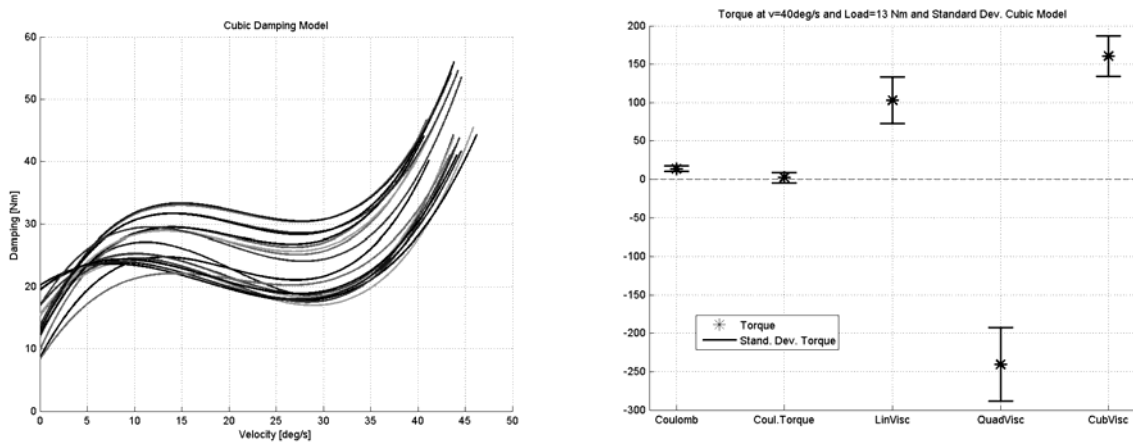| Description and Date	b_0 [Nm]	b_{0T} [-]	b_1 [Nm·s/rad]	b_2 [Nm·s²/rad²]	b_3 [Nm·s³/rad³]
On Ground Reference	7.573	0.127	168.388	-544.193	516.421
Spring 2005 03 24	12.372	0.146	163.301	-578.954	547.449
Spring 2005 05 12	10.850	-0.178	194.957	-608.227	570.378
Sinusoidal 2005 12 22	11.635	-	258.253	-1246.582	1805.827

Fig. 8. Simulated damping (left) and average contribution and bandwidth of damping terms (right) for several measurements during the entire mission (velocity = 40°/s and joint torque = 13Nm)
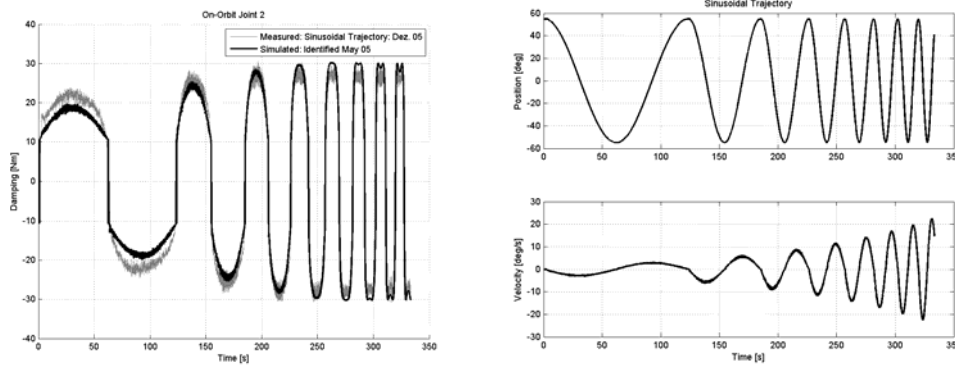
Fig. 9. Damping (left) of sinusoidal trajectory (right) simulated with parameters
identified for a different trajectory (spring 2005 05 12)

Mission Duration Dependency

The simulated damping torque in Fig. 7 indicates an increasing damping torque at low velocities. To study the time dependency of friction in detail, the average measured damping torque is calculated for different velocity ranges. The influence of the joint torque and the load dependent Coulomb friction respectively is not considered as all trajectories undergo the same load. For joint 1, the joint damping on ground is remarkable lower for all velocities than in space and therefore not considered in the following. For velocities between 4°/s and 6°/s the average damping torque of joint 2 is continuously increasing with time, including the on ground measurement (see Fig. 10). This suggests that the increased joint friction in space when compared to the ground values is partly related to the degeneration of the joints mechanical parts with time. For joint 1, damping tends to increase with time as well but with some isolated values. For higher velocities, e.g. in Fig. 11 between 27°/s and 35°/s, the average damping of each joint can be subdivided in two groups. The measurements taken during daytime and higher temperatures respectively differ from the measurements taken at lower temperatures. Each group shows a clear dependency on time. At higher velocities, damping increases with time and temperature. The temperature dependency for all velocities will be treated in the next subchapter.
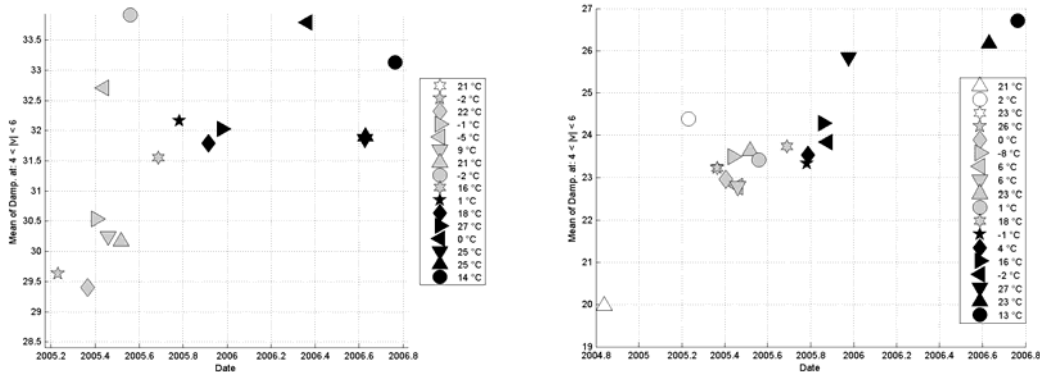

Fig. 10. Evaluation of average damping torque for joint 1 (left) and joint 2 (right): Velocity range 4°/s-6°/s
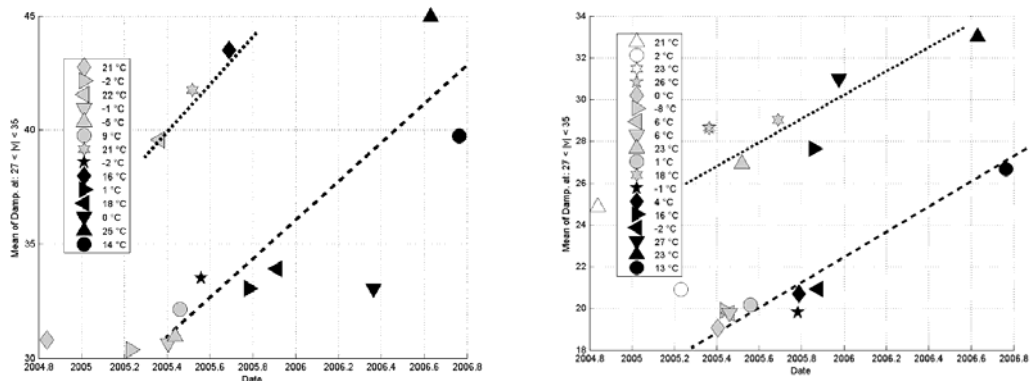(November 2004: on-ground reference)

Fig. 11. Evaluation of average damping torque for joint 1 (left) and joint 2 (right): Velocity range 27°/s-35°/s

Temperature Dependency

A heating system is used to regulate the operating temperatures on-orbit between -20°C and +30°C. The operating temperature within this range mainly depends on the solar radiation. During the short contact interval (3-7 minutes) and operation respectively, the temperature increases only slightly. The temperature is continuously measured at 5 points of each joint but none of them is placed exactly at the harmonic drive. The temperatures measured at different sensor locations differ only slightly and therefore the average temperature of all sensors is used. It can be assumed that this value represents a good estimation of the temperature inside the gear-box. Near zero velocity, the calculated average damping between 0.5°/s and 1.5°/s is depicted in Fig. 12, the average damping torque decreases significantly with temperature. For both joints, the average damping at 20°C is approximately 40% lower compared to the value at -5°C. With increasing velocity this effect disappears. In Fig. 13 it can be seen, that around 5°/s the temperature has almost no effect on the damping torque. At higher velocities, temperature has got a contrary effect on the damping. According to Fig. 14, the damping torque at around 25°C is approximately 40% higher than at -5°C. It can be stated that for both joints Coulomb damping decreases with temperature whereas the viscous damping increases.
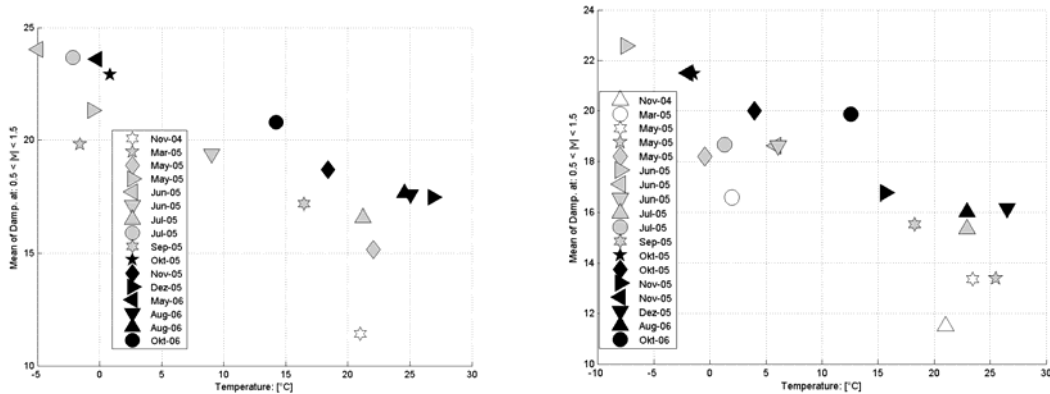
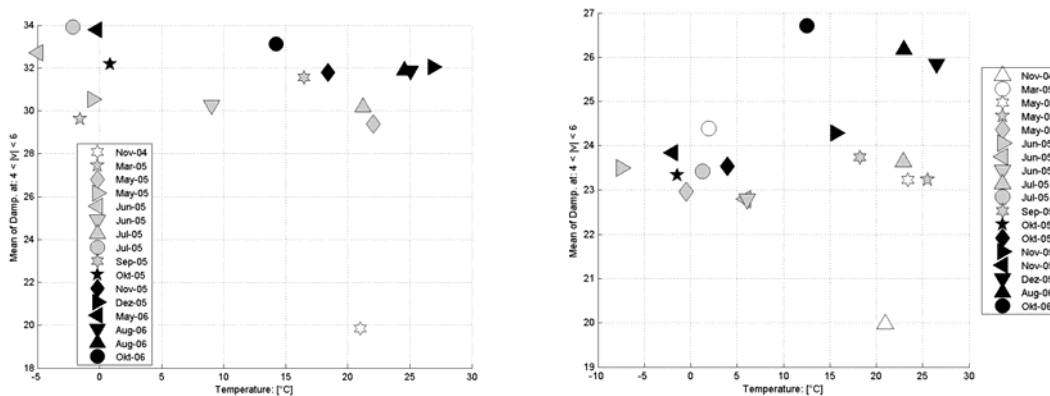Fig. 12. Temperature dependency near zero velocities for joint 1 (left) and joint 2 (right): Velocity range 0.5°/s-1.5°/s

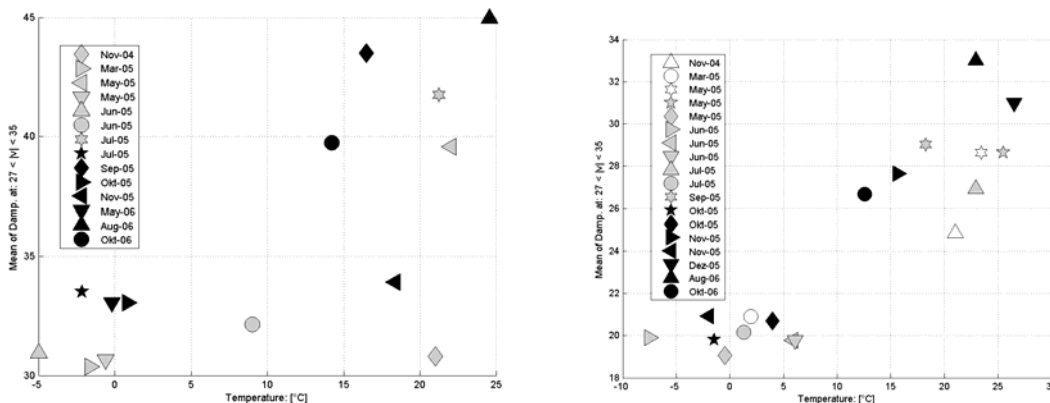Fig. 13. Temperature dependency at medium velocities for joint 1 (left) and joint 2 (right): Velocity range 4°/s-6°/s

Fig. 14. Temperature dependency at high velocities for joint 1 (left) and joint 2 (right): Velocity range 27°/s-35°/s

STIFFNESS IDENTIFICATION

The elasticity of the joints is basically defined by the stiffness of the flex spline of the harmonic drives and the torque sensor. Placing the pointer tip on the experimental contour, the elasticity of the stylus can be neglected, the joint position is fixed. Applying an increasing motor torque (saw tooth) the motor position represents the elastic deformation of the system. Since the torque is measured after the gear-box, the stiffness can be easily identified with the available torque and motor position signal. A typical identification result can be seen in Fig. 15. The stiffness for joint 2 has values around 4400 Nm/rad on-ground and 4900 Nm/rad in space. As expected, the stiffness identified in space almost matches the stiffness identified on-ground. For both joints, the observed change is below 15%.
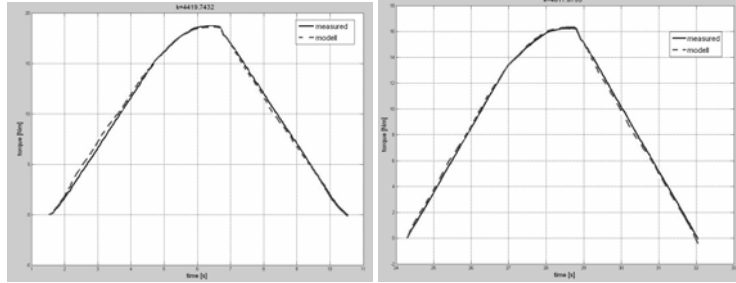

Fig. 15. Results of stiffness identification on ground (left) and on-orbit (right) for joint 2

CONTACT DYNAMICS EXPERIMENTS

To study how the space environment affects the behavior of bodies interacting together in a contact situation, the aluminium pointer tip of the stylus is moved along a straight edge of the experimental contour, while keeping the normal force constant. The same trajectories, sinusoidal motions with different frequencies and normal forces, are executed at a lubricated (dry-film lubricant) and an unlubricated surface (aluminium). Both the direction of the normal force $\mathbf{F}_N$, defined by the gradient $\nabla\Phi$ of the constraint surface and the direction of the tangential force $\mathbf{F}_T$ given by the velocity of the contact point $\dot{\mathbf{r}}_{ee}$ are known. The contact forces can be calculated by measuring the joint torques τ_1 and τ_2 and by considering the dynamics of the robot [8]:

$$
\frac{\mathrm{d}}{\mathrm{d}t}\left(\frac{\partial L}{\partial \dot{q}_1}\right) - \frac{\partial L}{\partial q_1} = \tau_1 + \left(F_N \nabla\Phi - F_T \frac{\dot{\mathbf{r}}_{ee}}{|\dot{\mathbf{r}}_{ee}|}\right)\frac{\partial \mathbf{r}_{ee}}{\partial q_1}
$$

$$
\frac{\mathrm{d}}{\mathrm{d}t}\left(\frac{\partial L}{\partial \dot{q}_2}\right) - \frac{\partial L}{\partial q_2} = \tau_2 + \left(F_N \nabla\Phi - F_T \frac{\dot{\mathbf{r}}_{ee}}{|\dot{\mathbf{r}}_{ee}|}\right)\frac{\partial \mathbf{r}_{ee}}{\partial q_2}
$$

(5)

For both contact surfaces the calculated tangential contact force is nearly constant and therefore a Coulomb type friction model is applied.

$$
F_T = b_{0T}\,|F_N|\cdot sign\left(\dot{q}_1\right)
$$

(6)

Typical results for the calculated contact forces are given in Fig. 16. Near zero velocity the tangential force takes on negative values. This is completely understandable. Due to the elasticity of the manipulator the pointer is still in rest while the measured motor position moves already backwards. Up to the point where the pointer tip starts to move the direction of the tangential force is not defined by the velocity of the motor position. Measurements taken near zero velocity are therefore ignored for parameter identification. Except for the first orbit, the pointer tip may have been contaminated, friction and the identified friction parameter respectively are nearly constant for the unlubricated surface. For the lubricated surface friction increases with time and slowly approaches the values obtained for the unlubricated surface. Typical results for both surfaces are given in Fig. 17. Further investigation of the contact case is in progress.
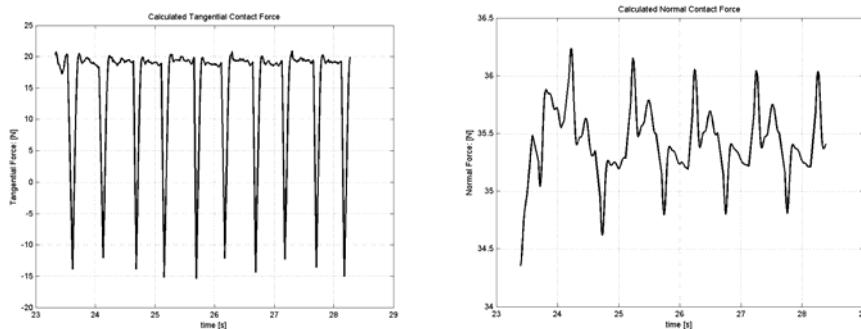

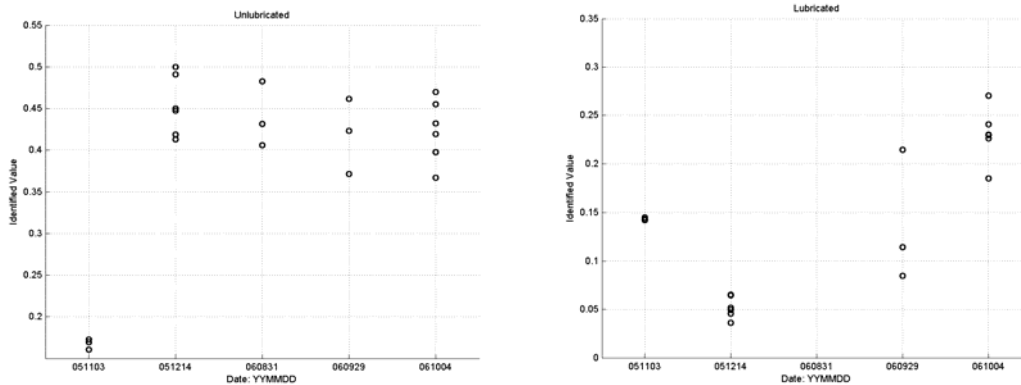Fig. 16. Calculated tangential (left) and normal (right) contact force

Fig. 17. Results for contact dynamics identification: Identified friction parameter for unlubricated (left) and lubricated (right) contact surface

CONCLUSION

Initially, it was planned to operate ROKVISS for one year. Within the first phase, all initial goals of the mission have been achieved [9]. The hardware proved to work reliably under space conditions and ROKVISS will be continued to study the long term effect in detail. Space qualified lubricants strongly affect the damping behavior and a nonlinear friction model has to be introduced. Friction continuously increases with time and strongly depends on temperature with different effects for slow and fast motions. The experiments were performed in blocks and during each mission block the measurements are taken around the same time of the day. To isolate the effect of mission time and temperature, measurements will be taken at different temperatures in short intervals and the temperature dependency will be included in the joint model. For further space missions temperature sensors should be placed close to the gear-box.

The dynamical parameters of the joints, mainly of joint 1, changed when the system was exposed to the outer space conditions. The two joints showed a slightly different behavior and the changes can not be completely explained by the temperature dependency. The majority of the developed hardware and the results of the experiments will be taken into account for the design of more complex free-flying robotic systems (e.g. 7-axis robots) and paved the way for more complex on-orbit servicing missions like Orbital Recovery, a first business case that deals with orbital recovery of malfunctioned satellites or with the extension of a satellite's lifetime [10].

REFERENCES

[1] Landzettel, K., Brunner, B., Lampariello, R., Preusche, C., Reintsema, G., et al., "System Prerequisites and Operational Modes for On Orbit Servicing", Proc. ISTS International Symposium on Space Technology and Science, Miyazaki, June 2004

[2] Schäfer, B., Landzettel, K., Albu-Schäffer, A., Hirzinger, G.:, "ROKVISS: Orbital Testbed for Tele-Presence Experiments, Novel Robotic Components and Dynamics Models Verification", Proc. 8th ESA Workshop on Advanced Space Technologies for Robotics and Automation (ASTRA), Noordwijk, November, 2004

[3] Schäfer, B., Rebele, B., Landzettel, K., "ROKVISS - Space Robotics Dynamics and Control Performance Experiments at the ISS", Proc. ACA2004 IFAC Symposium on Automatic Control in Aerospace, St. Petersburg, ,, pp.333-338, June 2004

[4] Preusche, C., Reintsema, D., Landzettel, K., Fischer, M., Hirzinger, G., "DLR on the way towards Telepresent On-Orbit Servicing.", Proc. Mechatronics & Robotics, 2004

[5] Preusche, C., Reintsema, D., Landzettel, K., Hirzinger, G., "ROKVISS - towards Telepresence Control in Advanced Space Missions", Proc. 3rd. International Conference on Humanoid Robots, Munich and Karlsruhe, Oct. 2003

[6] Albu-Schäffer, A., "Regelung von Robotern mit elastischen Gelenken am Beispiel der DLR-Leichtbauarme", Doctoral Thesis, TU München 2002

[7] A. Albu-Schäffer, G. Hirzinger, "Parameter identification and passivity based joint control for a 7 DOF torque controlled light weight robot", Proc. Int. Conf. on Robotics and Automation, Seoul, pp. 1087-1093 , 2001

[8] B. Schäfer, B. Rebele, A. Fenili; "Space Robotics Contact Dynamics Investigations and Numerical Simulations: ROKVISS", ROMANSY 2004 – 15th CISM-IFToMM Symposium on Robot Design, Dynamics and Control, 14-, Montreal, 2004

[9] K. Landzettel, A. Albu-Schäffer, B. Brunner, A. Beyer, G. Hirzinger., et al., "ROKVISS Verification of Advanced Light Weight Robotic Joints and Tele-Presence Concepts for Future Space Missions", in press

[10] D.R. Wingo, "Orbital Recovery's Responsive Commercial Space Tug for Life Extension Missions", AIAA 2nd Responsive Space Conference, Los Angeles, April, 2004